Human Aldose Reductase: p*K* of Tyrosine 48 Reveals the Preferred Ionization State for Catalysis and Inhibition†

Charles E. Grimshaw,*,‡ Kurt M. Bohren,§ Chung-Jeng Lai,‡ and Kenneth H. Gabbay§

Whittier Diabetes Program, Department of Medicine, University of California, San Diego, La Jolla, California 92093-0983, and Molecular Diabetes and Metabolism Section, Departments of Pediatrics and Cell Biology, Baylor College of Medicine, Houston, Texas 77030

Received March 13, 1995; Revised Manuscript Received August 18, 1995⊗

ABSTRACT: Detailed analyses of the pH variation of kinetic parameters for the forward aldehyde reduction and reverse alcohol oxidation reactions mediated by recombinant human aldose reductase, for inhibitor binding, and for kinetic isotope effects on aldehyde reduction have revealed that the p*K* value for the active site acid−base catalyst group Tyr48 is quite sensitive to the oxidation state of the bound nucleotide (NADPH or $NADP^+$) and to the presence or absence of the Cys298 sulfhydryl moiety. Thus, the Tyr48 residue of C298A mutant enzyme displays a p*K* value that ranges from 7.6 in the productive *E·$NADP^+$ complex that binds and reacts with alcohols to 8.7 in the productive *E·NADPH complex that binds and reacts with aldehyde substrates. For wild-type enzyme, Tyr48 in the latter complex displays a lower p*K* value of about 8.25. Assignment of the p*K* values was facilitated by the recognition and quantitation of the degree of stickiness of several aldehyde substrates in the forward reaction. The unusual pH dependence for $V_{aldehyde}/E_t$ and $^DV_{aldehyde}$, which decrease roughly 20-fold through a wave and remain constant at high pH, respectively, is shown to arise from the pH-dependent decrease in the net rate of $NADP^+$ release. The results described are fully consistent with the chemical mechanism for aldose reductase catalysis proposed previously (Bohren et al., 1994) and, furthermore, establish that binding of the spirohydantoin class of aldose reductase inhibitors, e.g., sorbinil, occurs via a reverse protonation scheme in which the ionized inhibitor binds preferentially to the *E·$NADP^+$ complex with Tyr48 present as the protonated hydroxyl form. The latter finding allows us to propose a unified model for high-affinity aldose reductase inhibitor binding that focuses on the transition state-like nature of the *E-Tyr48-OH·$NADP^+$·$inhibitor^-$ complex.

In 1994, Tyr48 was established as the active site acid−base catalytic residue for the reaction catalyzed by aldose reductase (AR)[1] and, by analogy, other members of the aldo−keto reductase superfamily (Bohren et al., 1994). The role of Tyr48 was established on the basis of site-directed mutagenesis, X-ray crystallographic, and kinetic findings on wild-type and mutant aldose reductase enzymes. A novel chemical mechanism was proposed in which hydride transfer from NADPH to the aldehyde substrate is facilitated via polarization of the carbonyl moiety by the hydroxyl group of Tyr48, whose apparent p*K* is shifted to a value of 8.4 by interaction within a hydrogen-bonding network comprised of Asp43 and Lys77. At the time, the p*K* value for Tyr48 was based on the p*K* of 8.4 determined from the log ($V/K_{glyceraldehyde}E_t$) versus pH profile, with an assumption that DL-glyceraldehyde was a nonsticky substrate, i.e., its dissociation from the productive *E·NADPH·aldehyde complex occurs faster than its reaction forward to give alcohol product. However, recent stopped-flow kinetic studies using D-xylose as a substrate indicate that aldehydes are sticky (Grimshaw et al., 1995a,b), and thus the true p*K* value for Tyr48 is likely to be lower than previously assigned. We have therefore reinvestigated the pH dependence of the kinetic parameters for both the aldehyde reduction and alcohol oxidation reactions mediated by recombinant human aldose reductase (hAR). We have also reexamined the pH dependence of inhibitor binding and kinetic isotope effects on aldehyde reduction, in order to resolve the issue of aldehyde substrate stickiness and determine the true p*K* of the catalytic Tyr48 residue in various productive enzyme complexes.

Previous attempts to conduct detailed pH studies using aldose reductase have been plagued by a number of technical difficulties. The low turnover number for AR has hampered pH studies which rely on large changes in both V/E_t and K_m values to establish important ionizing groups on the enzyme and substrate(s). In addition, a number of side reactions have been documented that can further compromise the accuracy

† This work was supported by NIH Grants DK 43595 (C.E.G.) and EY 11018 (K.H.G.), Juvenile Diabetes Foundation grants (K.M.B. and K.H.G.), and the Harry B. and Aileen B. Gordon Foundation (K.H.G.).

* Address correspondence to this author, at the University of California, San Diego, Whittier Diabetes Program, Department of Medicine 0983, 9500 Gilman Dr., La Jolla, CA 92093-0983. Phone: (619) 535-8037 or (619) 622-8422 (new); Fax: (619) 535-0894; Internet: cgrimshw@scripps.edu.

‡ University of California, San Diego.

§ Baylor College of Medicine.

⊗ Abstract published in *Advance ACS Abstracts,* October 15, 1995.

[1] Abbreviations: Na_2EDTA, disodium ethylenediaminetetraacetate; Mes, 2-(*N*-morpholino)ethanesulfonic acid; Mopso, 3-(*N*-morpholino)-2-hydroxypropanesulfonic acid; Popso, piperazine-*N*,*N*′-bis(2-hydroxypropanesulfonic acid); Capso, 3-(cyclohexylamino)ethanesulfonic acid; sorbinil (CP 45,634), (*S*)-2,3-dihydro-6-fluorospiro[4*H*-1-benzopyran-4,4′-imidazolidine]-2′,5′-dione; PCA, 1-pyrrolidinecarboxaldehyde; $NADP^+$, β-nicotinamide adenine dinucleotide phosphate; NADPH, reduced form of $NADP^+$; AR, aldose reductase; hAR, recombinant human aldose reductase; NADPD, (4*R*)-[4-^{2}H]NADPH; DTT, dithiothreitol; LADH, liver alcohol dehydrogenase; LDH, lactate dehydrogenase; ARI, aldose reductase inhibitor.

0006-2960/95/0434-14374$09.00/0

of initial rate measurements (Grimshaw, 1990; Grimshaw et al., 1990a). The presence of "activated" or "oxidized" forms of the enzyme, which occur naturally (Grimshaw & Lai, 1995) or can be produced during purification and storage of the native enzyme, has been a recurring problem because these modified enzyme forms often display drastically altered kinetic properties with respect to both substrates and inhibitors (Srivastava et al., 1985; Bhatnagar et al., 1989; Del Corso et al., 1989; Grimshaw et al., 1989; Vander Jagt & Hunsaker, 1993; Cappiello et al., 1994).

The C298A mutant hAR, by virtue of its resistance to oxidative modification, enhanced stability, and increased values for both turnover number and K_m value for the nucleotide cofactors (Grimshaw et al., 1995b), is ideally suited to the type of detailed pH studies required to resolve these questions relating to the chemical mechanism of aldose reductase catalysis. Recent kinetic studies (Petrash et al., 1992, 1993; Bohren & Gabbay, 1993; Bhatnagar et al., 1994) have established that Cys298 is largely responsible for the observed oxidative modulation of aldose reductase activity, consistent with the location of the Cys298 sulfhydryl group within the active site pocket as revealed by crystallographic studies of several E·NADP$^+$·anion complexes (Wilson et al., 1992; Harrison et al., 1994; Bohren et al., 1994). As we have shown (Grimshaw et al., 1995a,b), replacement of Cys298 with an alanine residue alters the rate of several steps along the reaction pathway. The rate constant for the enzyme conformational change occurring during nucleotide exchange is increased 8.7- and 17-fold for NADP$^+$ and NADPH, respectively, while the apparent rate constants for xylose binding and hydride transfer are decreased 5.5- and 2-fold, respectively, for the C298A mutant enzyme as compared to the wild-type enzyme. In the present paper, we have taken advantage of the unique stability and kinetic properties of the C298A mutant enzyme to evaluate the stickiness of aldehyde substrates and the pH dependence of substrate and inhibitor binding and of catalysis mediated by human aldose reductase. Our results reveal a strong dependence of the Tyr48 pK value on the oxidation state of the bound nucleotide and on the presence or absence of the cysteine sulfhydryl moiety. In addition, analysis of the pH profiles for both substrates and inhibitors offers new insight into the preferred protonation state of the active site Tyr48 residue required for optimal binding and catalysis, which should be useful in the design of more potent and specific aldose reductase inhibitors.

MATERIALS AND METHODS

With the exception of the methods outlined below, all other chemicals and methods have been described in the two preceding papers (Grimshaw et al., 1995a,b).

Assay Conditions. Unless otherwise noted, initial velocity and inhibition patterns were determined in 50 mM buffer consisting of 2-(*N*-morpholino)ethanesulfonic acid (Mes) (pH 5.5−6.5), Mopso (pH 6.5−7.5), Popso (pH 7.5−9.0), diethanolamine (pH 9.0−9.5), or ethanolamine (pH 9.5−10.5). Overlaps were used in all cases, and checks were made to ensure that the buffers used would neither inhibit nor activate the enzymic reaction.[2] Aldehyde reduction was normally followed by using a Cary 3 spectrophotometer and associated kinetic analysis software. Standard reaction mixtures contained saturating NADPH (100−200 μM) and variable concentrations of aldehyde. NADPH was added just prior to the addition of enzyme to start the reaction. In the direction of alcohol oxidation, or for full initial velocity patterns involving variation of both nucleotide and substrate concentration for either NADPH or NADP$^+$, reactions were monitored using a Spex Fluoromax photon-counting spectrofluorimeter, as described (Grimshaw et al., 1995a). Due to the sensitivity of the Spex instrument, nucleotide concentrations could readily be varied in the 0.2−5 μM range. Care was taken to ensure that the concentration of enzyme was always at least 10-fold lower than the lowest nucleotide concentration used to avoid problems associated with the extremely tight binding of nucleotides by hAR (Del Corso et al., 1990; Grimshaw et al., 1990b). For V/E_t and V/KE_t pH profiles, the nucleotide concentration was in all cases shown to be saturating (at least 10 × K_m). Each data point was determined in duplicate over at least 5 substrate concentrations. Control assays, lacking either substrate or enzyme, were routinely included, and the rates, if any, were subtracted from the observed reaction rates.

Data Processing. Reciprocal initial velocities were plotted versus reciprocal substrate concentrations, and the experimental data were fitted to eq 1−10 by the least-squares method, assuming equal variances for the v or log Y values

$$v = VA/(K + A) \quad (1)$$

$$v = VA/[K(1 + I/K_{is}) + A] \quad (2)$$

$$v = VA/[K + A(1 + I/K_{ii})] \quad (3)$$

$$v = VA/[K(1 + I/K_{is}) + A(1 + I/K_{ii})] \quad (4)$$

$$v = VA/[K(1 + F_iE_{V/K}) + A(1 + F_iE_V)] \quad (5)$$

$$v = VAB/[K_aB(1 + F_iE_{V/Ka}) + AB(1 + F_iE_V) + K_b(A + K_{ia})(1 + F_iE_{V/Kb})] \quad (6)$$

$$\log Y = \log[C/(1 + H/K_1)] \quad (7)$$

$$\log Y = \log[C/(1 + K_2/H)] \quad (8)$$

$$\log Y = \log[C/(1 + H/K_1 + K_2/H)] \quad (9)$$

$$\log Y = \log\{[Y_L + Y_H(K_2/H)]/(1 + K_2/H)\} \quad (10)$$

(Wilkinson, 1961), and using the Fortran programs of Cleland (1979). The points in the figures are the experimentally determined values, while the curves are calculated from fits of these data to the appropriate equation. Linear double-reciprocal plots were fitted to eq 1. Data conforming to linear competitive, uncompetitive, and noncompetitive inhibition were fitted to eqs 2, 3, and 4, respectively. Data for kinetic deuterium isotope effects[3] when one substrate was

[2] Ethanolamine derivatives were used for assays above pH 9 since we discovered that the Capso buffer used in previous pH studies at pH 9.5−10.0 (Bohren et al., 1994) displays competitive inhibition versus xylitol and uncompetitive inhibition versus xylose (K_i = 15 mM at pH 9.5).

[3] The isotope effect nomenclature used is that of Northrop (1977) and Cleland (1987) in which a leading superscript indicates the isotope effect being studied. Thus, ^DV, $^DV/K$, and ^Dk are primary deuterium isotope effects on V/E_t, V/KE_t, and k, respectively.

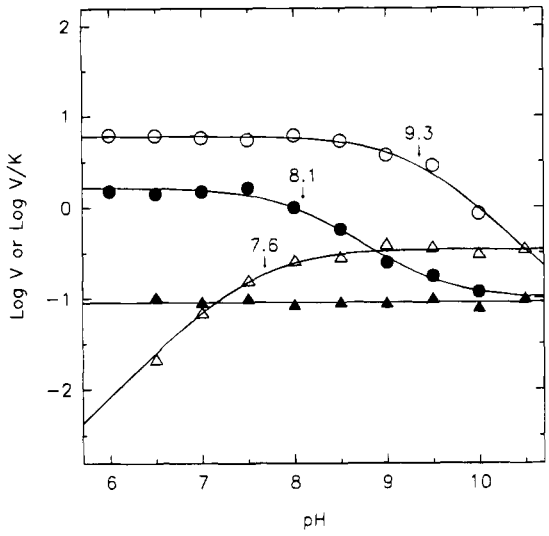

FIGURE 1: pH profiles for the forward and reverse reactions catalyzed by C298A mutant hAR with D-xylose and D-xylitol as the variable substrate, respectively. $\log(V_{xylose}/E_t)$ (●), $\log(V/K_{xylose}E_t)$ (○), $\log(V_{xylitol}/E_t)$ (▲), $\log(V/K_{xylitol}E_t)$ (△). The units of V/E_t are s^{-1}, and those of V/KE_t are M^{-1} s^{-1}. Curves and pK values shown were calculated from fits to eq 7, 8, or 10, as described under Results.

varied were fitted to eq 5, where F_i is the fraction of deuterium in the nucleotide, $E_{V/K}$ and E_V are the isotope effects minus 1 on V/KE_t and V/E_t, respectively, and A is the concentration of the substrate used. Equation 6 was used when isotope effects were seen on V/E_t, V/K_aE_t (K_a = K_{NADPH}), and V/K_bE_t (K_b = $K_{aldehyde}$) in a sequential mechanism where full initial velocity patterns were determined with deuterated and unlabeled nucleotide cofactors.

Data for pH profiles were fitted to eqs 7−10, which describe respectively a log Y versus pH curve that decreases with unit slope below pK_1 (eq 7); decreases with a slope of −1 above pK_2 (eq 8); decreases both below pK_1 and above pK_2 with slopes of +1 and −1, respectively (eq 9); and shows two plateau values (Y_L at low pH; Y_H at high pH), with pK_2 being the point where Y is the average of the two plateau values (eq 10). In eqs 7−10, H is the hydronium ion concentration ([H^+]), and C is the pH-independent value of Y at the optimal state of protonation.

RESULTS

pH Profiles for Aldehyde Reduction and Alcohol Oxidation. As shown in Figure 1 and tabulated in Table 1, pH profiles for $V/K_{xylose}E_t$ and $V/K_{xylitol}E_t$ with C298A mutant enzyme displayed reciprocal behavior, with the former decreasing a factor of 10 per pH unit above a pK of 9.3 ± 0.1 and the latter decreasing a factor of 10 per pH unit below a pK of 7.6 ± 0.1. This is the behavior expected for the acid−base catalytic group that facilitates hydride transfer in both directions, previously identified as Tyr48 (Bohren et al., 1994). V_{xylose}/E_t displayed a wave decreasing 19-fold above a pK of 8.1 ± 0.1. $V_{xylitol}/E_t$, however, was pH-independent over the range pH 6.5−10.5, with a value of 0.090 ± 0.005 s^{-1}. pH profiles qualitatively similar to those described for C298A-mediated reduction of D-xylose were observed for reduction of DL-glyceraldehyde using either enzyme (Figure 2), except that the pK values determined for wild-type enzyme were routinely shifted to lower pH by about 0.6 unit. $V_{glyceraldehyde}/E_t$ for each enzyme again displayed a wave, decreasing an average of 25-fold above an apparent pK value of 7.0 ± 0.2 for wild-type and 7.7 ± 0.3 for C298A mutant enzyme, respectively.

pH Profiles for Dead-End Inhibition with C298A Mutant hAR. The pK_i versus pH profiles for three dead-end inhibitors versus D-xylose or D-xylitol are shown in Figure 3, and the corresponding pK and limiting K_i values are listed in Table 1. Inhibition patterns versus D-xylose or xylitol were in each case measured at a saturating concentration of nucleotide cofactor. 1-Pyrrolidinecarboxaldehyde (PCA), an

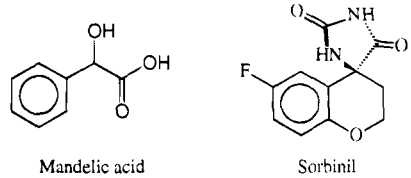

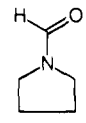

1-Pyrrolidine carboxaldehyde (PCA)

uncharged amide analogue of the aldehyde substrate, displayed linear noncompetitive inhibition versus D-xylose. The pK_{is} value (equal to $-\log K_{is}$) determined for the competitive inhibition component from fits to eq 4 decreased through a wave above an apparent pK of 8.7 ± 0.1, with an overall 4.5-fold drop in binding affinity on the high pH plateau (Figure 3). Thus, binding of the neutral PCA molecule to the *E·NADPH binary complex is favored when Tyr48 is present as the protonated hydroxyl form. The pK_{ii} value for the intercept component of PCA inhibition versus D-xylose, found to be equal within experimental error to the pK_{is} value for purely competitive inhbition by PCA versus xylitol in the reverse reaction, thus represents PCA binding to the *E·NADP$^+$ complex. Furthermore, because the pK_{is} versus pH curve for competitive inhibtion by PCA versus xylitol is flat, PCA binding to the binary *E·NADP$^+$ complex must not be affected by the protonation state of Tyr48, in contrast to the results obtained for PCA binding to *E·NADPH. Binding of the simple organic acid DL-mandelic acid, which also displayed purely competitive inhibition versus xylitol in the reverse reaction, was similarly diminished upon deprotonation of Tyr48 with an apparent pK of 7.8 ± 0.2 in the *E·NADP$^+$ complex. The magnitude of the wave in pK_{is} value for DL-mandelic acid (pK_a 3.4), which is present as the carboxylate anion over the entire pH range studied, corresponds to a 20-fold preference for inhibitor binding when Tyr48 is protonated. Versus D-xylose at pH 8.0, DL-mandelic acid displayed essentially uncompetitive inhibition, and fitting the data to eq 3 gave a K_{ii} value (6 mM) equal to the K_{is} for competitive inhibition versus xylitol (data not shown). Fitting the same data to eq 4 to detect any slope effect in the inhibition by DL-mandelate versus D-xylose indicated that the K_{is} value for binding to *E·NADPH must be at least 10-fold greater than the K_{ii} value determined for binding of the monoanionic inhibitor to *E·NADP$^+$.

Sorbinil, which displayed linear uncompetitive inhibition versus D-xylose and linear competitive inhibition versus xylitol (data not shown), gave essentially superimposable bell-shaped pK_{ii} and pK_{is} versus pH profiles, respectively,

Table 1: Comparison of pK and Plateau Values Determined from the pH Variation of Kinetic Parameters for Recombinant Wild-Type and C298A Mutant Human Aldose Reductase

parameter	eq fitted	pK_1	pK_2	C[a]
		C298A Mutant, Forward Reaction		
$\log(V/K_{xylose}E_t)$	8		9.3 ± 0.1	6.1 ± 0.3 M^{-1} s^{-1}
$\log(V/K_{glyceraldehyde}E_t)$	8		9.0 ± 0.1	9000 ± 400 M^{-1} s^{-1}
$\log(V_{xylose}/E_t)$	10		8.1 ± 0.1	1.9 ± 0.1; 0.10 ± 0.01 s^{-1}
$\log(V_{glyceraldehyde}/E_t)$	10		7.7 ± 0.3	2.3 ± 0.1; 0.10 ± 0.01 s^{-1}
$pK_{is\ PCA}$ vs xylose[b]	10		8.7 ± 0.1	20 ± 1; 93 ± 5 mM
$pK_{ii\ sorbinil}$ vs xylose	9	7.4 ± 0.1	8.7 ± 0.1	53 ± 10 nM
$^DV/K_{glyceraldehyde}$	10		8.4 ± 0.2	1.84 ± 0.02; 2.37 ± 0.05
		C298A Mutant, Reverse Reaction		
$\log(V/K_{xylitol}E_t)$	7	7.6 ± 0.1		0.35 ± 0.02 s^{-1}
$\log(V_{xylitol}/E_t)$	c			0.090 ± 0.005 s^{-1}
$pK_{is\ sorbinil}$ vs xylitol	9	7.4 ± 0.2	8.8 ± 0.1	81 ± 9 nM
$pK_{is\ mandelate}$ vs xylitol	10	7.8 ± 0.2		2.5 ± 0.4; 47 ± 8 mM
$pK_{is\ PCA}$ vs xylitol	c			45 ± 5 mM
		Wild-Type, Forward Reaction		
$\log(V/K_{glyceraldehyde}E_t)$	8		8.4 ± 0.1	12 900 ± 600 M^{-1} s^{-1}
$\log(V_{glyceraldehyde}/E_t)$	10		7.0 ± 0.2	0.73 ± 0.03; 0.038 ± 0.002 s^{-1}

[a] For pK_i profiles, eqs 9 and 10 were used with $Y = 1/K_i$. The value tabulated for C is K_i, however, not $1/K_i$. For eq 10, the V/E_t, K_i, or isotope effect value at low pH is given first, followed by the high pH value. [b] Inhibition is noncompetitive; the curve for the intercept effect (pK_{ii}) is flat and equal to the pK_{is} versus xylitol curve. [c] pH-independent value.

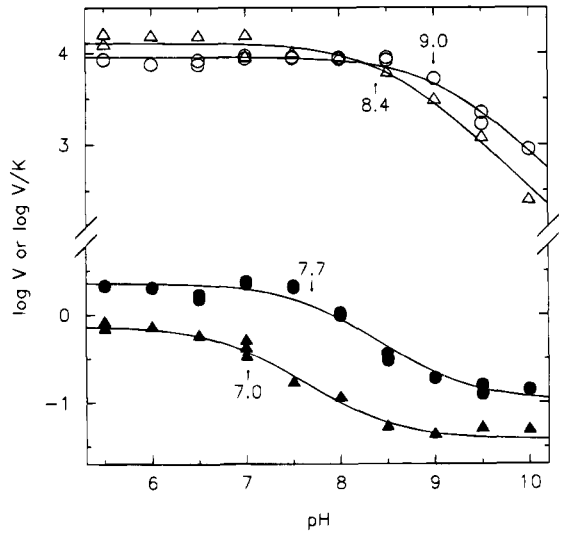

FIGURE 2: pH profiles for the forward direction catalyzed by wild-type and C298A mutant hAR with DL-glyceraldehyde as the variable substrate. Wild-type hAR: $\log(V/E_t)$ (▲), $\log(V/KE_t)$ (△); C298A mutant hAR: $\log(V/E_t)$ (●), $\log(V/KE_t)$ (○). The units of V/E_t are s^{-1}, and those of V/KE_t are M^{-1} s^{-1}. Curves and pK values shown were calculated from fits to eq 8 or 10.

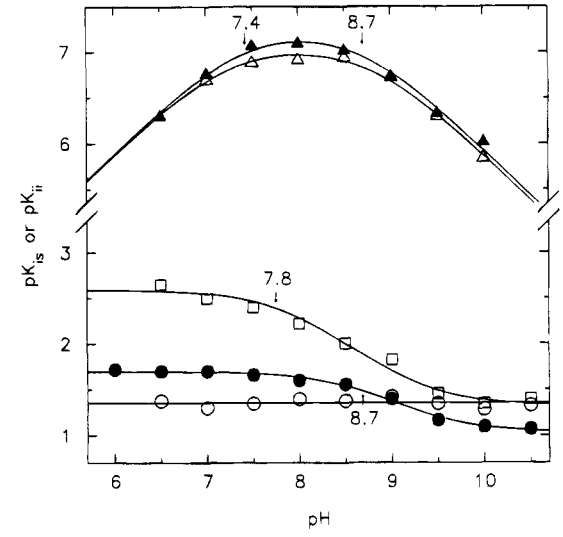

FIGURE 3: pK_i profiles in the forward and reverse directions catalyzed by C298A mutant hAR with D-xylose and D-xylitol as the variable substrate, respectively. $pK_{ii\ sorbinil}$ vs D-xylose (▲), $pK_{is\ sorbinil}$ vs D-xylitol (△), $pK_{is\ mandelate}$ vs D-xylitol (□), $pK_{is\ PCA}$ vs D-xylose (●), $pK_{is\ PCA}$ vs D-xylitol (○) (equal to $pK_{ii\ PCA}$ vs D-xylose). The units of K_i are M. Curves and pK values shown were calculated from fits to eq 9 or 10.

with apparent pK values of 7.4 ± 0.1 on the acidic side and 8.7 ± 0.1 on the basic side. Sorbinil also displayed linear uncompetitive inhibition versus $NADP^+$ in the reverse reaction, and the apparent K_{ii} value increased with increasing concentration of xylitol as expected if the inhibitor binds only to the productive *E·$NADP^+$ complex (data not shown). Thus, the pK of 7.8 and 7.4 determined for inhibition by DL-mandelate and sorbinil, respectively, versus xylitol and the pK of 7.6 observed for $V/K_{xylitol}E_t$ must be the true pK for Tyr48 in the productive *E·$NADP^+$ complex. Likewise, the pK of 8.7 determined for the competitive component of PCA inhibition versus D-xylose represents the true pK for Tyr48 in the productive *E·NADPH complex.

pH Profiles for Isotope Effects. Primary deuterium isotope effects determined for C298A mutant hAR by direct comparison of initial velocities measured at a saturating concentration of NADPH or NADPD with DL-glyceraldehyde as the variable substrate are plotted as a function of pH in Figure 4. As shown, $^DV/K_{glyceraldehyde}$ increased through a wave as the pH increased, while $^DV_{glyceraldehyde}$ remained flat or showed a slight decrease. A fit to eq 10 of the $^DV/K_{glyceraldehyde}$ data yielded an apparent pK value (8.4 ± 0.2) close to that determined from the $\log(V/K_{glyceraldehyde}E_t)$ profile (9.0 ± 0.1). Note that even at pH 10 the $^DV_{glyceraldehyde}$ value did not fall below 1.00 and thus did not approach the equilibrium isotope effect value, $^DK_{eq}$ = 0.93 (Cook et al., 1980). Although not as complete as the C298A mutant data, a similar trend was noted for wild-type enzyme, with $^DV/K_{glyceraldehyde}$ increasing from 1.71 at pH 5.5 to 1.98 at pH 10, while $^DV_{glyceraldehyde}$ remains essentially constant.

Isotope Effects on Initial Velocity Patterns. Isotope effects on the kinetic parameters V_{xylose}/E_t, $V/K_{xylose}E_t$, and $V/K_{NADPH}E_t$ for C298A mutant enzyme were obtained from fits to eq 6 (or to a similar equation in which the logarithm is taken

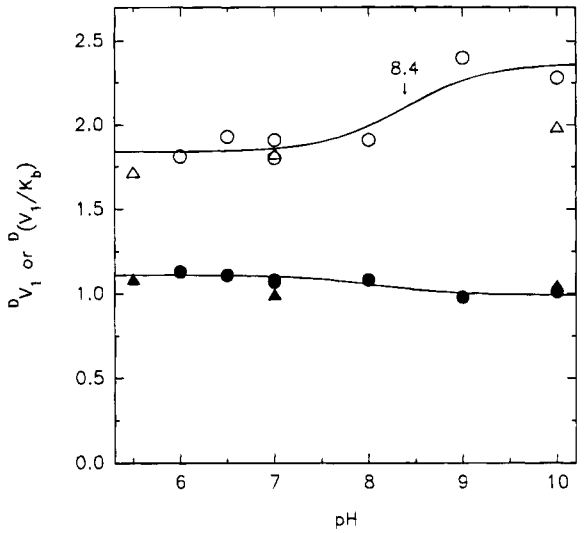

FIGURE 4: pH variation of deuterium isotope effects for wild-type and C298A mutant hAR determined by direct comparison with DL-glyceraldehyde as the variable substrate at saturating NADPH or NADPD. Curves and pK values shown were calculated from fits to eq 10 of $^{D}V_{glyceraldehyde}$ and $^{D}V/K_{glyceraldehyde}$ values determined from fits of initial velocity data to eq 5. $^{D}V/K_{glyceraldehyde}$: wild-type (△), C298A (○); $^{D}V_{glyceraldehyde}$: wild-type (▲), C298A (●).

Table 2: Kinetic Isotope Effects for C298A Mutant hAR Determined by Direct Comparison of Initial Velocity Patterns with NADPH and NADPD

parameter	D-xylose[a]	DL-glyceraldehyde[b]
$^{D}V_{aldehyde}$	1.07 ± 0.02	1.08 ± 0.01
$^{D}V/K_{aldehyde}$	2.70 ± 0.09	1.91 ± 0.04
$^{D}V/K_{NADPH}$	1.01 ± 0.05	1.00 ± 0.03

[a] Sodium phosphate buffer, pH 8.0. [b] Mops buffer, pH 7.0.

of both sides) of the entire data set determined at pH 8 consisting of the complete initial velocity patterns for both NADPH and NADPD (each pattern contained 20 duplicate data points determined at four fixed concentrations of NADPH/D and five variable concentrations of aldehyde substrate). These results and those from a similar study using DL-glyceraldehyde and wild-type enzyme at pH 7 are listed in Table 2. In each case, the observed value of $^{D}V/K_{NADPH}$ was not significantly different from unity, and thus the kinetic reaction must be strictly ordered, with NADPH binding first, followed by aldehyde substrate (see below).

DISCUSSION

As a result of extensive X-ray crystallographic and site-directed mutagenesis studies, the active site residue Tyr48 was identified as the acid−base catalyst which donates a proton in the aldehyde reduction reaction and accepts a proton in the alcohol oxidation reaction mediated by recombinant human aldose reductase (Harrison et al., 1994; Bohren et al., 1994). The reciprocal behavior with pH observed in the log(V/KE_t) versus pH profiles shown in Figure 1 for reaction of D-xylose and xylitol in the forward and reverse reaction directions catalyzed by C298A mutant enzyme, respectively, is fully consistent with this assignment. Thus, Tyr48 must be protonated for aldehyde reduction and ionized for alcohol oxidation, with the overall active site maintaining a net zero overall charge. We include in this global charge the positive charge on the nicotinamide ring of $NADP^+$ and the $Lys77^+$−$Asp43^-$ couple that should

Scheme 1

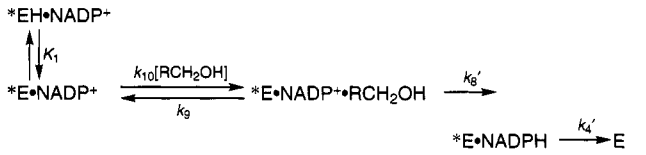

remain overall electroneutral over the pH range studied. Reduction of DL-glyceraldehyde by either wild-type or C298A mutant aldose reductase displays a similar pH dependence to that seen with D-xylose (Figure 2). Through a detailed analysis of the pH dependence of the kinetic parameters for substrate binding and catalysis, inhibitor binding, and kinetic isotope effects, we can now assign pK values for the crucial Tyr48 residue in the various productive complexes of both wild-type and C298A mutant aldose reductase.

pH Profiles for Xylitol Oxidation and Xylose Reduction by C298A Mutant Enzyme. The pH behavior for reaction in the direction of xylitol oxidation is analyzed first since it fits the simplest model. As shown in Figure 1, log($V/K_{xylitol}E_t$) decreases at low pH below a simple pK of 7.6. $V_{xylitol}/E_t$, on the other hand, is pH-independent over the entire range of pH 10.5−6.5. Essentially the same pK value of 7.8 is observed for the binding of the competitive inhibitor DL-mandelate (Figure 3), but in this case binding is lost at high pH rather than at low pH as we observe for the substrate xylitol. The same pK value of 7.4 is also seen for competitive inhibition by sorbinil, although this pH profile is more complex and will be analyzed in more detail below. The fact that the same pK value of 7.6 ± 0.2 is seen in both the $V/K_{xylitol}E_t$ and pK_{is} profiles for the competitive inhibitors indicates that this represents the true pK value for Tyr48 in the productive *E•$NADP^+$ complex of the C298A mutant enzyme and, furthermore, that xylitol is not a sticky substrate. The latter fact is consistent with the results obtained from stopped-flow studies conducted at pH 8 (Grimshaw et al., 1995b).

The observed pH dependence of the kinetic parameters for xylitol oxidation is best described by the model in Scheme 1, in which binding of the alcohol substrate (RCH_2OH) and catalysis can only proceed via the *E•$NADP^+$ complex in which the Tyr48 group is unprotonated. The sequence of steps leading up to *E•$NADP^+$ is not included because $NADP^+$ is saturating for all the pH profiles in question. The rate constant numbering scheme is taken directly from the preceding papers (Grimshaw et al., 1995a,b), and K_1 is the acid dissociation constant for Tyr48 in the binary *EH•-$NADP^+$ complex. Net rate constants (Cleland, 1975) are used for the catalytic sequence ($k_8' = k_8k_6/(k_7 + k_6)$, including hydride transfer and release of the aldehyde product) and for NADPH release ($k_4' = k_4k_2/(k_2 + k_3)$).

Assignment of the pK value in the productive *EH•NADPH complex has been more problematic. Previously, a pK value of 8.4 was assigned to the ionization of Tyr48 in this complex based on the observed pK in the log($V/K_{glyceraldehyde}E_t$) profile and an assumption that the aldehyde substrate was not sticky (Bohren et al., 1994). Stopped-flow studies using D-xylose have now clearly demonstrated that aldehyde substrates are indeed sticky for both wild-type and C298A mutant enzyme (Grimshaw et al., 1995a,b). Unfortunately, a suitable competitive inhibitor versus the aldehyde substrate was not available at the time these pH studies were initiated.

Scheme 2

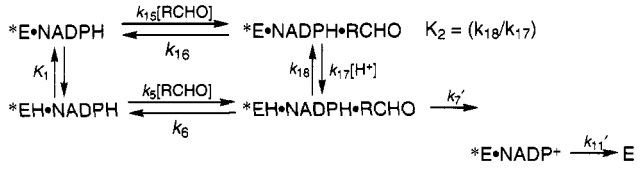

Menadione has been reported as a competitive inhibitor versus aldehyde substrates for both aldose and aldehyde reductase (Bhatnagar et al., 1988, 1991), but in our hands this compound was ineffective. After screening a number of simple aromatic and aliphatic amides and esters containing a carbonyl moiety to mimic that of the substrate, we selected 1-pyrrolidinecarboxaldehyde (PCA) as an effective inhibitor versus the aldehyde substrate.

Comparison of the $\log(V/K_{xylose}E_t)$ profile for C298A mutant enzyme (Figure 1) with the pK_{is} profile for the competitive component of inhibition by PCA versus D-xylose (Figure 3) confirms that D-xylose is a sticky substrate. Thus, the pK of 9.3 in the $\log(V/K_{xylose}E_t)$ profile is shifted 0.6 unit to higher pH from the true pK of 8.7 seen for the competitive inhibitor. Because the stickiness of the aldehyde substrate results in a shift in the pK observed in the $\log(V/K_{aldehyde}E_t)$ profile, the reaction in the forward direction is best described by the model of Cook and Cleland (1981b), as shown in Scheme 2, in which the aldehyde substrate (RCHO) can bind to the enzyme whether or not Tyr48 is protonated (*E or *EH), but catalysis can only proceed when this group is protonated (*EH). The rate constant numbering scheme is again taken directly from the preceding papers (Grimshaw et al., 1995a,b) with the addition of steps for Tyr48 protonation in and RCHO binding to the *E•NADPH complex, and where $K_2 = k_{18}/k_{17}$ is the acid dissociation constant for the ternary *EH•NADPH•RCHO complex. Because $k_8 \ll k_9$ (Grimshaw et al., 1995a,b), the net rate constant $k_7' = k_7k_9/(k_8 + k_9) \approx k_7$. The 0.6 unit p$K$ shift we observe for D-xylose reduction by C298A mutant enzyme corresponds to a stickiness ratio (k_7/k_6) of 3.0 ($\Delta pK = \log(1 + k_7/k_6)$ (Cleland, 1977)), which compares favorably with the k_7/k_6 ratio of 2.3 determined from stopped-flow studies at pH 8 (Grimshaw et al., 1995b). For DL-glyceraldehyde reduction the pK shift is only 0.3 unit, which corresponds to a stickiness ratio of $k_7/k_6 \approx 1$.

To corroborate the stickiness ratios for C298A mutant enzyme and to obtain an estimate for the true pK value for Tyr48 in wild-type enzyme where the relevant competitive inhibition pH profiles are not available, we turn to the pH variation of $^DV/K_{aldehyde}$:

$$^DV/K_{aldehyde} = (^Dk_7 + C_f + C_r{}^DK_{eq})/(1.0 + C_f + C_r) \quad (11)$$

where $^Dk_7$ is the maximum observable isotope effect,[4] $C_r = k_8/k_9 \approx 0$ (Grimshaw et al., 1995a,b) is the reverse commitment factor, and the pH dependence derives from the apparent decrease in the forward commitment factor ($C_f = k_7/k_6$) as Tyr48 becomes ionized at high pH and the effective concentration of the productive *EH•NADPH complex decreases. Thus, 1 pH unit below the pK of 8.7 for C298A mutant enzyme, essentially all the enzyme will be present as the protonated Tyr48-OH form required for aldehyde reduction, the value of $C_f = k_7/k_6$ will be maximal, and the observed $^DV/K_{aldehyde}$ value will be minimal. Conversely, 1 pH unit above the pK of 8.7, most of the enzyme will be in the ionized Tyr48-O$^-$ form which is not competent for aldehyde reduction, and the effective k_7 value and thus the C_f value will be very low, with the result that $^DV/K_{aldehyde} \approx {}^Dk_7$. The difference in $^DV/K_{aldehyde}$ values on the low pH and high pH plateaus thus provides another estimate for the stickiness ratio. Comparing the $^DV/K_{glyceraldehyde}$ value for C298A mutant enzyme (Figure 4) on the high pH plateau (2.37) with that on the low pH plateau (1.82), we calculate a value for C_f of 0.67 which compares well with the value of 1 estimated by the pK shift method. A similar analysis using the pH variation of $^DV/K_{glyceraldehyde}$ for wild-type enzyme (Figure 4) gives a stickiness ratio of 0.38 for DL-glyceraldehyde which would correspond to a pK shift of 0.15 unit. Thus, the true pK for Tyr48 in the wild-type *EH•NADPH complex must be equal to 8.4−0.15 ≅ 8.25, or roughly 0.45 pH unit lower than the pK determined for C298A mutant enzyme.

The results described herein for human AR can be compared with an earlier pH study of bovine AR, in which Liu et al. (1993) reported a simple pK of 7.5 in both the $\log(V_{aldehyde}/E_t)$ and $\log(V/K_{aldehyde}E_t)$ profiles using *p*-chlorobenzaldehyde as the substrate. However, because data were collected only up to pH 8, the wave in $\log(V_{aldehyde}/E_t)$ we observe for either wild-type or C298A mutant human enzyme may have been misinterpreted as ionization of the active site acid−base catalyst. For reaction in the reverse reaction, the bovine enzyme displayed a pK of 7.5 in the $\log(V/K_{alcohol}E_t)$ profile using *p*-chlorobenzyl alcohol as the substrate, similar to our results for xylitol (Figure 1), but the $\log(V_{alcohol}/E_t)$ profile again displayed a break below a pK of 6.5. On the basis of the similar pK values of 7.5 for the $\log(V/KE_t)$ profiles for reaction in each direction, these authors concluded that the identity of the bound nucleotide (e.g., NADPH versus NADP$^+$) had little effect on the pK value for the active site acid−base catalytic residue. By contrast, our results clearly indicate that when NADP$^+$ is bound, the pK for Tyr 48 is further shifted to lower pH by an additional 1.1 units from the value of 8.7 seen in the *EH•NADPH complex, a value which is itself shifted about 1.8 units down from the pK of 10.5 seen for free tyrosine in solution. The presence of the cysteine sulfhydryl of Cys298 in the wild-type enzyme accounts for about a 0.45 pK unit shift toward stabilizing the ionized form of Tyr48 relative

[4] Given $^Dk_7 \approx 6.5$ for D-xylose reduction (Grimshaw et al.,1995a,b), the apparent $^Dk_7$ value for DL-glyceraldehyde reduction is likely not the intrinsic effect and may be reduced from this value by "internal" commitment factors (Cook & Cleland, 1981a). Thus, if k_7 consists of a sequence of steps:

$$*E\cdot NADPH\cdot RCHO \underset{k_{26}}{\overset{k_{25}}{\rightleftharpoons}} {}^{\diamond}E\cdot NADPH\cdot RCHO \underset{k_{28}}{\overset{k_{27}}{\rightleftharpoons}}$$

$$^{\diamond}E\cdot NADP^+\cdot RCH_2OH \underset{k_{30}}{\overset{k_{29}}{\rightleftharpoons}} *E\cdot NADP^+\cdot RCH_2OH \xrightarrow{k_9}$$

including pre- (k_{25}, k_{26}) and post-catalytic (k_{29}, k_{30}) conformational changes as well as the isotope-dependent hydride transfer step (k_{27} and k_{28}), then k_7 and $^Dk_7$ will be given by:

$$k_7 = (k_{25}k_{27}/k_{26})/[1.0 + (k_{27}/k_{26}) + (k_{28}/k_{29})(1.0 + (k_{30}/k_9))]$$

$$^Dk_7 = [^Dk_{27} + C_f + C_r{}^DK_{eq}]/[1.0 + C_f + C_r]$$

where $^DK_{eq} = {}^Dk_{27}/{}^Dk_{28}$ is the equilibrium effect, $C_r = (k_{28}/k_{29})[1.0 + (k_{30}/k_9)]$ and $C_f = k_{27}/k_{26}$ are the reverse and forward "internal" commitment factors, respectively, and $^Dk_{27}$ is the intrinsic deuterium isotope effect on hydride transfer.

to the pK of 8.7 observed for the *EH·NADPH complex of the C298A mutant enzyme in which the -SH moiety is replaced by a hydrogen atom.

At this time, it is premature to assign a single structural basis for the observed pK shifts. The enhanced perturbation of the pK for Tyr48 in the wild-type enzyme relative to the C298A mutant can be correlated with an increase in the extent of clamping observed for nucleotide binding to the respective enzymes as monitored by stopped-flow methods (Grimshaw et al., 1995a,b). Several careful crystallographic studies (Wilson et al., 1992, 1993; Harrison, et al., 1994; Bohren et al., 1994) show that the Cys298 sulfhydryl moiety and the hydroxyl group of Tyr48 are in close proximity to the C4-position of the nicotinamide ring within the enzyme active site. Yet, in each of the crystal structures studied to date, the nucleotide cofactor in the "locked" enzyme configuration is $NADP^+$ which is bound in the presence of an anionic species (Harrison et al., 1994; Bohren et al., 1994; Ehrig et al., 1994). It remains to be established whether the relationship of active site residues to each other and to the nicotinamide are similar in an NADPH crystal form of the enzyme. Structurally, the interaction of the sulfhydryl group of Cys298 with the nucleotide enfolding loop and the nucleotide appears to be a key interaction (Gabbay et al., unpublished). The crystallographic data are thus consistent with the conclusion from our stopped-flow kinetic studies that modification of the Cys298 thiol group leads to a weaker interaction with the nucleotide enfolding loop.

Anomalous pH Behavior of $V_{aldehyde}/E_t$ and ${}^DV_{aldehyde}$. The model in Scheme 2 cannot, however, account for the wave we observe in the log($V_{aldehyde}/E_t$) profile for xylose with C298A or for DL-glyceraldehyde with either wild-type or C298A mutant enzyme. A wave could result if both the protonated (*EH·NADPH·RCHO) and unprotonated (*E·NADPH·RCHO) ternary complexes were catalytically competent, with the latter showing a 20-fold lower turnover number. In that case, however, the log($V/K_{aldehyde}E_t$) profile would also show a wave. A more likely explanation is another pH-dependent step outside the catalytic sequence comprising $V/K_{aldehyde}E_t$ that becomes slower by a factor of 20 as the pH is increased. Previously, we ascribed this wave to a net decrease in the rate of $NADP^+$ release at high pH (Bohren et al., 1994), and thus we have modified the kinetic model for aldehyde reduction, as shown in Scheme 3, to include a second ionizable group (shown by a preceding H, as in *HE) that controls the net rate of $NADP^+$ release. Hence, k_{11}' is the net rate constant for $NADP^+$ release from the protonated enzyme (*HE) at low pH, while k_{19}' is the corresponding rate constant at high pH.

In order to understand the pH variation of $V_{aldehyde}/E_t$, we begin with the following equation, which describes $V_{aldehyde}/E_t$ as a function of pH according to Scheme 2 (Cleland, 1977):

$$V_{aldehyde}/E_t = k_7'/[1 + (k_7'/k_{11}') + (K_2/H)] \quad (12)$$

and which displays asymptotes to the curve at low and high pH that cross at pK_{app} given by:

$$pK_{app} = pK_2 + \log[1 + (k_7'/k_{11}')] \quad (13)$$

The only assumption made in the derivation of eq 12 is that $k_{17} \gg V_{aldehyde}/E_t$, which for hAR implies that $k_{17} \gg k_{11}'$, a good assumption given how rate-limiting $NADP^+$ release has been shown to be (Grimshaw et al., 1995a,b). Assuming for the moment that pK_2 = pK_1 = 8.7, eq 13 predicts that the pK observed in the log($V_{aldehyde}/E_t$) profile will be shifted to higher pH by the kinetic factor log[1 + (k_7'/k_{11}')]. We know from stopped-flow studies with C298A mutant enzyme at pH 8 that $k_7'/k_{11}' \approx 38$ (Grimshaw et al., 1995b), which translates into a pK_{app} value of at least 10.3. Next, we take into account the slowing of $NADP^+$ release at high pH by substituting the expression for $k_{11}'_{,19}'$:

Scheme 3

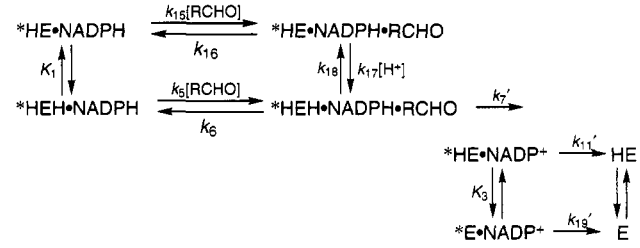

$$k_{11}'_{,19}' = [k_{11}' + k_{19}'(K_3/H)]/[1.0 + (K_3/H)] \quad (14)$$

in place of k_{11}' in eq 13. Equation 14 resembles eq 10 in form, with the value decreasing from k_{11}' at low pH through a wave above pK_3 to a value equal to k_{19}' at high pH. Since we know that k_{19}' is about 20-fold slower than k_{11}', the break in the log($V_{aldehyde}/E_t$) profile will not appear until pK_{app} of 11.6! Thus far, we have only collected data up to pH 10.5 and have not yet detected any break in log(V_{xylose}/E_t) due to Tyr48 ionization. We cannot therefore determine either the pK_2 value or the effect of Tyr48 ionization on the relative binding affinity of the aldehyde substrate.

The model in Scheme 3 can also account for the pH variation of ${}^DV_{aldehyde}$ shown in Figure 4. Again, we start with an equation for ${}^DV_{aldehyde}$ derived for Scheme 2:

$${}^DV_{aldehyde} = ({}^Dk_7 + C_{Vf} + C_r{}^DK_{eq})/(1.0 + C_{Vf} + C_r) \quad (15)$$

where $C_r = k_8/k_9 \approx 0$ (Grimshaw et al., 1995a,b) and C_{Vf} is given by the following expression:

$$C_{Vf} = (k_7/k_{11}')/[1 + (K_2/H)] \quad (16)$$

Substituting $k_{11}'_{,19}'$ from eq 14 in place of k_{11}' in eq 16 yields:

$$C_{Vf} = [k_7\{1.0 + (K_3/H)\}]/[\{1.0 + (K_2/H)\}\{k_{11}' + k_{19}'(K_3/H)\}] \quad (17)$$

where essentially the same pK_3 value (8.1 ± 0.1) controls the wave seen in the log(V_{xylose}/E_t) profile (Figure 1) and that (7.7 ± 0.3) observed for DL-glyceraldehyde reduction (Figure 2). According to eq 17, as C_{Vf} increases above pK_3 ≈ 8 from a value equal to k_7/k_{11}' on the low pH plateau to a value equal to k_7/k_{19}' on the high pH side of the break in $V_{glyceraldehyde}/E_t$, the observed ${}^DV_{glyceraldehyde}$ for the C298A mutant enzyme should decrease to a value very close to unity at high pH. Assuming a value of k_7/k_{11}' for reduction of DL-glyceraldehyde equal to the ratio $k_7/k_{11}' \approx 38$ determined using D-xylose at pH 8 (Grimshaw et al., 1995b), and recognizing that $V_{glyceraldehyde}/E_t$ at pH 8.0 is already down about 2-fold from the optimal rate at low pH, the ${}^DV_{glyceraldehyde}$ values calculated using eq 15 are 1.07 at low pH and 1.00 on the high pH plateau. Thus, the predicted behavior for

$^{D}V_{glyceraldehyde}$ as a function of pH is consistent with what we observe experimentally (Figure 4). As the pH continues to increase above $pK_{app} \approx 11.6$, $V_{glyceraldehyde}/E_t$ should start to decrease and $^{D}V_{glyceraldehyde}$ to increase as the ionization of Tyr48 results in the catalytic sequence becoming rate-limiting for the overall reaction, until eventually $^{D}V_{glyceraldehyde}$ becomes equal to the maximum observed $^{D}V/K_{aldehyde} \approx 2.37$.

Several examples have been reported in the literature where, despite an increase in both $^{D}V/K$ and ^{D}V beyond the break in the pH profiles as predicted by Scheme 2, the increase in ^{D}V plateaus at a value that is lower than the maximum $^{D}V/K$ value. In each case, this unusual behavior has been ascribed to a slow, pH-dependent step occurring outside of the sequence of steps comprising V/KE_t for the substrate. For instance, in the oxidative deamination of alanine catalyzed by alanine dehydrogenase, the rate of isomerization of the initial E·NAD$^+$ complex to a form that can productively bind alanine and proceed through catalysis is largely rate-limiting at neutral pH. The rate constant for this conformational change decreases a factor of 10 per pH unit at low pH, just as does the net rate constant for the hydride transfer sequence. Thus, below the break in the log-($V_{alanine}/E_t$ profile, the isotope effects on both $^{D}V/K_{alanine}$ and $^{D}V_{alanine}$ increase, but $^{D}V_{alanine}$ plateaus at a value (1.35) significantly less than that for $^{D}V/K_{alanine}$ (1.97) (Grimshaw & Cleland, 1981). Yet, to our knowledge, hAR is the first example of a dehydrogenase where ^{D}V remains constant, or even decreases slightly at the same time that the $^{D}V/K$ value is increasing beyond the break in the log(V/KE_t) profile.

At present, we have not assigned pK_3 to the ionization of any particular residue in the protein structure. Recently, Srivastava and co-workers have addressed this question using solvent perturbation methods and concluded that the high pH "break" in the log($V_{aldehyde}/E_t$) profile derives from ionization of a cationic acid such as histidine (Liu et al., 1994). Unfortunately, because they ascribe this same pK to the active site residue involved in acid−base catalysis of the hydride transfer reaction, they cite these results as evidence that His110, and not Tyr48, serves this function in aldose reductase. We now understand that the "break" in the log-($V_{aldehyde}/E_t$) profile is really a wave and, furthermore, that the pH variation of $^{D}V_{aldehyde}$ is not consistent with pK_3 being assigned to ionization of the active site catalytic residue. Rather, the lack of an increase in $^{D}V_{aldehyde}$ above pK_3 must result from an increase in the extent of rate limitation by a second, pH-dependent step that lies outside the catalytic sequence of steps that comprise $V/K_{aldehyde}E_t$. However, the results of Liu et al. (1994) do suggest that the rate of nucleotide exchange for both wild-type and C298A mutant enzyme may indeed by modulated by ionization of another His or Lys residue which remains to be identified.

Practical Consequences of the Kinetic Mechanism. Analysis of the kinetic model clearly shows that for both wild-type and C298A mutant hAR the predominant enzyme form during steady-state turnover of aldehyde reduction is *E·NADP$^+$ (Grimshaw et al., 1995a,b). Thus, a linear competitive inhibitor versus xylitol should be a linear uncompetitive inhibitor versus D-xylose, and the K_{is} and K_{ii} values should be nearly equal. In addition, because the decrease in $V_{aldehyde}/E_t$ at high pH results from a slowing in the net rate of NADP$^+$ release for both wild-type and C298A mutant enzyme, the near equivalence of K_{ii} and K_{is} should hold over a wide range of pH. Data for inhibition by both sorbinil and PCA (comparing pK_{ii} versus D-xylose with pK_{is} versus xylitol) confirm that this is the case (Figure 3). To our knowledge, this is the first demonstration for an aldose reductase inhibitor of an equivalence for the K_{ii} for inhibition versus aldehyde and the K_{is} for inhibition versus alcohol over a wide pH range. That these compounds act as competitive inhibitors versus the alcohol substrate in the back-reaction by binding to the E·NADP$^+$ complex was previously shown in studies of both aldose and aldehyde reductase (Wermuth, 1991; Liu et al., 1992; Harrison et al., 1994; Ehrig et al., 1994). Ward and co-workers (Ward et al., 1993) in a study of biphasic inhibition kinetics suggested that most, if not all, aldose reductase inhibitors function by binding to a putative "E*·Q" complex which is, in fact, equivalent to our *E·NADP$^+$ complex.

The same kinetic rationale suggests why there are no known aldose reductase inhibitors that show other than competitive inhibition versus the alcohol substrate. During steady-state turnover for alcohol oxidation, very little enzyme is present as the *E·NADPH complex, while during steady-state turnover in the opposite direction virtually all the enzyme is present as the *E·NADP$^+$ complex. Thus, compounds that bind effectively to either *E·nucleotide complex (e.g., PCA in Figure 3) will show noncompetitive inhibition versus the aldehyde substrate, but only competitive inhibition versus the alcohol substrate. The apparent K_i value for inhibitor binding to a particular enzyme form is given by:

$$\text{app } K_i = (\text{true } K_i)/(E_i/E_t) \quad (18)$$

where E_i is the concentration of the enzyme form to which the inhibitor binds and E_t is the sum total of all enzyme forms. Thus, if E_i is less than 1% of E_t, the apparent K_i value for binding to E_i will be so high as to preclude detection of inhibitor binding by steady-state kinetic studies. Such is the case for binding of aldose reductase inhibitors to *E·NADPH when studied in the direction of alcohol oxidation.

Ordered Reaction Mechanism. Work from other laboratories has suggested a random kinetic mechanism for aldehyde reduction mediated by AR isolated from several different mammalian species, based on the observation of a significant primary deuterium isotope effect on $V/K_{NADPH}E_t$ (Bhatnagar et al., 1988, 1994). In a strictly ordered bi-bi kinetic mechanism, Cook and Cleland (1981a) have shown that the V/K isotope effect for the first substrate to add must be equal to unity since extrapolation to a saturating concentration of the second substrate increases the forward commitment factor (C_f in the following equation):

$$^{D}V/K_{NADPH} = (^{D}k_7 + C_f + C_r{}^{D}K_{eq})/(1.0 + C_f + C_r) \quad (19)$$

to such a level that the maximum observable isotope effect[4] on the hydride transfer step is completely masked. As shown in Table 2, the isotope effect on $V/K_{NADPH}E_t$ measured by direct comparison of full initial velocity patterns for both DL-glyceraldehyde and D-xylose is not significantly different from unity, and thus aldehyde reduction mediated by aldose reductase must follow a strictly ordered kinetic mechanism. This conclusion is entirely consistent with the stopped-flow results, which suggest that it is only *after* NADPH has bound that the enzyme is able to undergo the necessary structural reorganization to form an active site configuration capable

of aldehyde reduction. The discrepancy in ${}^{D}V/K_{NADPH}$ values likely derives from the questionable practice of using high concentrations of sulfate ion (0.4 M) in the assay buffer to enhance the reaction velocity (Srivastava et al., 1985; Bhatnagar et al., 1988, 1989, 1994). The reported K_m and K_i values for NADPH and $NADP^+$ under such assay conditions are extremely high (30−48 μM) as compared with the submicromolar values determined in our studies (Grimshaw et al., 1995a,b) and elsewhere (Del Corso et al., 1989; Ehrig et al., 1994). The practice of using high sulfate ion concentrations should not be employed for detailed kinetic and mechanistic studies since monovalent and multivalent anions have been shown to both inhibit and activate the reactions catalyzed by aldose reductase in both directions (Hayman & Kinoshita, 1965; Grimshaw et al., 1989; Bohren et al., 1991; Harrison et al., 1994). Under such conditions, the kinetic mechanism becomes random, and thus, kinetic results obtained with the use of sulfate are suspect.

Inhibitor Binding and Preferred Ionization States. We next address the preferred protonation state of the Tyr48 residue and the various inhibitors as determined from dead-end inhibition studies as a function of pH and place these results in the context of the normal catalytic reaction mechanism. The neutral aldehyde analogue inhibitor PCA displays linear noncompetitive inhibition versus D-xylose with a K_{ii} value identical to the K_{is} obtained as a linear competitive inhibitor versus xylitol (Figure 3). Within a factor of about 4, PCA binds to either *E·$NADP^+$ or *E·-NADPH with about equal affinity, but it is only in the latter complex where PCA binding is sensitive to the protonation state of Tyr48, preferring, as does the aldehyde substrate, to bind when Tyr48 is protonated. The 4.5-fold decrease in binding affinity (increase in K_{is} value) for PCA inhibition versus D-xylose upon deprotonation of Tyr48 provides a good estimate of the relative binding affinity of the substrate for the two protonation states in Scheme 2. The fact that PCA binding is not affected by ionization of Tyr48 in the *E·-$NADP^+$ complex merely reinforces the idea that the relative contribution of various active site residues (e.g., Tyr48, His110, Trp111, Cys298, etc.) to the alignment and binding of both substrates and inhibitors may well be different depending on whether NADPH or $NADP^+$ is bound.

Binding of the simple organic acid DL-mandelate is clearly favored when Tyr48 is protonated, as evidenced by the 20-fold increase in K_{is} value (decrease in pK_{is}) for competitive inhibition versus xylitol as the pH is increased (Figure 3). On the basis of the nearly uncompetitive pattern obtained for inhibition versus D-xylose at pH 8, we can estimate that binding of DL-mandelate to *E·$NADP^+$ is favored at least 10-fold relative to binding to *E·NADPH. This is particularly surprising since, given the pK value for Tyr48 in the respective *E·nucleotide complexes, at pH 8 the $NADP^+$ complex (pK 7.6) will be mostly present in the less favored *E-Tyr48-O^-·$NADP^+$·$mandelate^-$ form, while the NADPH complex (pK 8.7) will be mostly in the favored *E-Tyr48-OH·NADPH·$mandelate^-$ form. Thus, despite an overall active site charge of −1 in each of the two complexes, binding of the mandelate anion is still favored by 10-fold when $NADP^+$ is the bound nucleotide. Combining these two factors results in a 200-fold preference for mandelate binding in the optimal *E-Tyr48-OH·$NADP^+$·$mandelate^-$ with Tyr48 protonated and an overall net active site charge of zero relative to the *E-Tyr48-OH·NADPH·$mandelate^-$ complex with NADPH bound and an overall net charge of −1. As we will discuss in more detail below, we ascribe the 200-fold stabilization of an enzyme complex with the stoichiometry *E-Tyr48-OH·$NADP^+$·$anion^-$ as a small indication of the transition state stabilization which enables aldose reductase to catalyze the efficient reduction of a broad spectrum of aldehyde substrates.

The pH profile for sorbinil inhibition is bell-shaped with pK values of 7.4 and 8.7, and thus the most potent inhibition (highest pK_i value) occurs between these two pKs. The obvious interpretation, and that preferred by Srivastava and co-workers who published a similar pH profile for sorbinil inhibition versus *p*-chlorobenzyl alcohol (Liu et al., 1992), is that the neutral form of sorbinil (pK of 8.4−8.7, depending on solvent polarity; Sarges et al., 1988) binds to the enzyme only when the active site Tyr48 is ionized. However, the bell-shaped pH profile can also occur as the result of a "reverse protonation" scheme (Cleland, 1977) in which exactly the opposite combination, namely, sorbinil anion bound to the enzyme with a protonated Tyr48, gives rise to the observed inhibition. These two possible configurations (sorbinil^0 plus *E-Tyr48-O^-·$NADP^+$ versus $sorbinil^-$ plus *E-Tyr48-OH^0·$NADP^+$) will display identical bell-shaped pH profiles, with the latter, less prevalent combination present at a level equal to $10^{(pK_1-pK_2)} = 10^{-1.3}$ or only 5% of the total. Equation 18 thus predicts that the true K_i will be 20-fold lower than the observed value, i.e., in the 2.5−4 nM range, which compares favorably with values for the most potent aldose reductase inhibitors (Dvornik, 1987)!

If one could test the equivalent of sorbinil anion at pH 6.6 where the Tyr48 residue in *E·$NADP^+$ is completely protonated, the K_{is} value measured would be in the nanomolar range. Much more is involved, however, than simply binding an anion at the enzyme active site, since DL-mandelate anion shows at best a binding constant (2 mM at pH 6.5) that is 1000-fold weaker than the best aldose reductase inhibitors. The recent crystal structure showing the potent aldose reductase inhibitor zopolrestat bound to the E·$NADP^+$ complex of human AR confirms not only that the carboxylate moiety is bound in precisely the location predicted (Harrison et al., 1994) but, furthermore, that a large number of interactions between enzyme and bound inhibitor, including van der Waals contacts and hydrogen bonds, combine to explain the high binding affinity for this compound (Wilson et al., 1993; Ehrig et al., 1994). Such is likely to be the case for the whole class of inhibitors based on the phenylacetic acid pharmacophore. Yet, recognition that sorbinil, as a representative of the spirohydantoin family of inhibitors, also inhibits by combining as the anionic species with the *E·$NADP^+$ complex enables us to propose a unified model for aldose (and, by analogy, aldehyde) reductase inhibitor action.

In chemical terms, the preference for binding anionic compounds when Tyr48 is present as the neutral -OH form makes perfect mechanistic sense. Catalysis of pyruvate reduction by lactate dehydrogenase relies on significant polarization of the carbonyl group in the E·NADH·pyruvate complex prior to hydride transfer (Deng et al., 1994). Binding at the active site via the carboxylate moiety further enhances the enzyme's ability to restrict the conformational freedom of the substrate so the optimal geometry for carbonyl polarization and subsequent hydride transfer can be attained. Similarly, aldehyde reduction by liver type alcohol dehy-

drogenase relies on polarization and conformational restriction of the substrate carbonyl group via coordination to the active site Zn^{2+} ion (Pettersson, 1987). We can assume that aldose reductase, which does not have the advantage of either a divalent metal ion or a substrate carboxylate tether, must still facilitate in some manner the polarization of the carbonyl group prior to or in concert with the hydride transfer step. Thus, in the transition state there should be a partial negative charge on the substrate oxygen with the proton that was formerly attached to the hydroxyl moiety of Tyr48 now partially bonded to both the substrate and the Tyr48 phenolic oxygen atom. For catalysis of aldehyde reduction, the transition state is reached via an initial *E-Tyr48-OH·RCHO·NADPH complex, while for alcohol oxidation the initial complex consists of *E-Tyr48-O^-·RCH_2OH·$NADP^+$. Binding of a monoanionic compound as an *E-Tyr48-OH·$NADP^+$·$anion^-$ complex thus resembles the transition state configuration derived by binding the uncharged alcohol substrate to the enzyme with Tyr48 ionized; the only difference is that catalysis can proceed in the latter complex, but not in the former. Essentially the same type of transition state analogue complex can be formed with lactate dehydrogenase when oxalate binds preferentially to the E·NAD^+ complex in which the catalytic histidine residue is protonated (Winer & Schwert, 1959; Holbrook & Gutfreund, 1973). The fact that some compounds, such as PCA (Figure 3) and alrestatin (Ehrig et al., 1994), show a competitive inhibition component versus aldehyde substrate, and thus can also bind to the *E-Tyr48-OH·NADPH complex, simply means that the active site can accommodate these structures. However, only complexes that contain the transition state analogue configuration—namely, *E-Tyr48-OH·$NADP^+$·$anion^-$—will display the tight binding properties. By the same reasoning, our results suggest that the transition state for aldose reductase-catalyzed aldehyde reduction will lie far toward alcoholate formation, at least with respect to proton transfer. The large solvent isotope effect observed for DL-glyceraldehyde reduction by wild-type hAR at neutral pH ($^{D_2O}V/K_{glyceraldehyde} = 4.73 \pm 0.23$; Bohren et al., 1994) is consistent with such a transition state structure. In addition, recent studies of the H112Q mutant of the closely related human aldehyde reductase have convincingly demonstrated that when catalysis is forced to occur in a discrete stepwise manner, hydride transfer to generate the bound alcoholate species occurs prior to the proton transfer step (Barski et al., 1995).

The aldose reductase active site has evolved to function as an excellent reductase but a very poor alcohol dehydrogenase. To a large extent, this effectively one-way catalysis is accomplished by a mechanism involving changes in the active site configuration that depend on the oxidation state of the bound nucleotide, as well as the presence of the sulfhydryl group of Cys298 which modulates interaction with a sophisticated nucleotide enfolding loop. Determination of the pK value and preferred ionization state for the catalytic Tyr48 residue, by means of pH studies of substrate and inhibitor binding, catalysis, and isotope effects, has clarified the mechanism for the normal reaction and provided insight into the high-affinity binding of aldose reductase inhibitors in a complex that resembles the transition state for hydride transfer. This improvement in our conceptual understanding should resolve several prevalent contradictions and ambiguities and should enable the development of specific and potent aldose reductase inhibitors.

REFERENCES

Barski, O. A., Gabbay, K. H., Grimshaw, C. E., & Bohren, K. M. (1995) *Biochemistry 34*, 11264−11275.

Bhatnagar, A., Das, B., Gavva, S. R., Cook, P. F., & Srivastava, S. K. (1988) *Arch. Biochem. Biophys. 261*, 264−274.

Bhatnagar, A., Liu, S.-Q., Das, B., & Srivastava, D. K. (1989) *Mol. Phamacol. 36*, 825−830.

Bhatnagar, A., Das, B., Liu, S.-Q., & Srivastava, S. K. (1991) *Arch. Biochem. Biophys. 287*, 329−336.

Bhatnagar, A., Liu, S.-Q., Ueno, N., Chakrabarti, B., & Srivastava, S. K. (1994) *Biochim. Biophys. Acta 1205*, 207−214.

Bohren, K. M., & Gabbay, K. H. (1993) in *Enzymology and Molecular Biology of Carbonyl Metabolism 4* (Weiner, H., Ed.) pp 267−277, Plenum Press, New York.

Bohren, K. M., Page, J. L., Shankar, R., Henry, S. P., & Gabbay, K. H. (1991) *J. Biol. Chem. 266*, 24031−24037.

Bohren, K. M., Grimshaw, C. E., Lai, C.-J., Harrison, D. A., Ringe, D., Petsko, G. A., & Gabbay, K. H. (1994) *Biochemistry 33*, 2021−2032.

Cappiello, M., Voltarelli, M., Giannessi, M., Cecconi, I., Camici, G., Manao, G., Del Corso, A., & Mura, U. (1994) *Exp. Eye Res. 58*, 491−501.

Cleland, W. W. (1975) *Biochemistry 14*, 3220−3224.

Cleland, W. W. (1977) *Adv. Enzymol. Relat. Areas Mol. Biol. 45*, 273−388.

Cleland, W. W. (1979) *Methods Enzymol. 63*, 103−138.

Cleland, W. W. (1987) in *Isotopes in Organic Chemistry* (Buncel, E., & Lee, C. C., Eds.) Vol. 7, Elsevier, Chapter 2, Amsterdam.

Cook, P. F., & Cleland, W. W. (1981a) *Biochemistry 20*, 1790−1796.

Cook, P. F., & Cleland, W. W. (1981b) *Biochemistry 20*, 1797−1805.

Cook, P. F., Blanchard, J. S., & Cleland, W. W. (1980) *Biochemistry 19*, 4853−4858.

Del Corso, A., Barsacchi, D., Giannessi, M., Tozzi, M. G., Camici, M., & Mura, U. (1989) *J. Biol. Chem. 264*, 17653−17655.

Del Corso, A., Barsacchi, D., Giannessi, M., Tozzi, M. G., Camici, M., Houben, J. L., Zandomeneghi, M., & Mura, U. (1990) *Arch. Biochem. Biophys. 283*, 512−518.

Deng, H., Zheng, J., Clarke, A., Holbrook, J. J., Callender, R., & Burgner, J. W., II (1994) *Biochemistry 33*, 2297−2303.

Dvornik, D. (1987) in *Aldose Reductase Inhibition: An Approach to the Prevention of Diabetic Complications* (Porte, D., Ed.) pp 222−323, McGraw Hill, New York.

Ehrig, T., Bohren, K. M., Prendergast, F. G., & Gabbay, K. H. (1994) *Biochemistry 33*, 7157−7165.

Grimshaw, C. E. (1990) *Enzymology and Molecular Biology of Carbonyl Metabolism 3* (Weiner, H., Ed.) pp 217−228, Plenum Press, New York.

Grimshaw, C. E., & Cleland, W. W. (1981) *Biochemistry 20*, 5655−5661.

Grimshaw, C. E., & Lai, C.-J. (1995) *Arch. Biochem. Biophys.* (submitted).

Grimshaw, C. E., Shahbaz, M., Jahangiri, G., Putney, C. G., McKercher, S. R., & Mathur, E. J. (1989) *Biochemistry 28*, 5343−5353.

Grimshaw, C. E., Shahbaz, M., & Putney, C. G. (1990a) *Biochemistry 29*, 9936−9946.

Grimshaw, C. E., Shahbaz, M., & Putney, C. G. (1990b) *Biochemistry 29*, 9947−9955.

Grimshaw, C. E., Bohren, K. M., Lai, C.-J., & Gabbay, K. H. (1995a) *Biochemistry 34*, 14356−14365.

Grimshaw, C. E., Bohren, K. M., Lai, C.-J., & Gabbay, K. H. (1995b) *Biochemistry 34*, 14366−14373.

Harrison, D. H., Bohren, K. M., Ringe, D., Petsko, G. A., & Gabbay, K. H. (1994) *Biochemistry 33*, 2011−2020.

Hayman, S., & Kinoshita, J. H. (1965) *J. Biol. Chem. 240*, 877−882.

Holbrook, J. J., & Gutfreund, H. (1973) *FEBS Lett. 31*, 157−169.

Liu, S.-Q., Bhatnagar, A., & Srivastava, S. K. (1992) *Biochem. Pharmacol. 44*, 427−429.

Liu, S.-Q., Bhatnagar, A., & Srivastava, S. K. (1993) *J. Biol. Chem. 268*, 25494−25499.
Liu, S.-Q., Bhatnagar, A., Ansari, N. H., & Srivastava, S. K. (1994) *FASEB J. 8*, A936.
Northrop, D. B. (1977) in *Isotope Effects on Enzyme-Catalyzed Reactions* (Cleland, W. W., O'Leary, M. H., & Northrop, D. B., Eds.) pp 122−152, University Park Press, Baltimore.
Petrash, J. M., Harter, T. M., Devine, C. S., Olins, P. O., Bhatanagar, A., Liu, S.-Q., & Srivastava, S. K. (1992) *J. Biol Chem. 267*, 24833−24840.
Petrash, J. M., Harter, T. M., Tarle, I., & Borhani, D. (1993) *Enzymology and Molecular Biology of Carbonyl Metabolism 4* (Weiner, H., Ed.) pp 289−300, Plenum Press, New York.
Pettersson, G. (1987) *CRC Crit. Rev. Biochem. 21*, 349−389.
Sarges, R., Schnur, R. C., Belletire, J. L., & Peterson, M. J. (1988) *J. Med. Chem. 31*, 230−243.
Sato, S., & Kador, P. F. (1990) *Biochem. Pharmacol. 40*, 1033−1042.
Srivastava, S. K., Hair, G. A., & Das, B. (1985) *Proc. Natl. Acad. Sci. U.S.A. 82*, 7222−7226.
Vander Jagt, D. L., & Hunsaker, L. A. (1993) *Enzymology and Molecular Biology of Carbonyl Metabolism 4* (Weiner, H., Ed.) pp 279−288, Plenum Press, New York.
Ward, W. H. J., Cook, P. N., Mirrlees, D. J., Brittain, D. R., Preston, J., Carey, F., Tuffin, D. P., & Howe, R. (1993) *Adv. Exp. Med. Biol. 328*, 301−311.
Wermuth, B. (1991) *Adv. Exp. Med. Biol. 284*, 197−204.
Wilkinson, G. N. (1951) *Biochem. J. 80*, 324−332.
Wilson, D. K., Bohren, K. M., Gabbay, K. H., & Quiocho, F. A. (1992) *Science 251*, 81−84.
Wilson, D. K., Tarle, I., Petrash, J. M., & Quiocho, F. A. (1993) *Proc. Natl. Acad. Sci. U.S.A. 90*, 9847−9851.
Winer, A. D., & Schwert, G. W. (1959) *J. Biol. Chem. 234*, 1155−1161.

BI9505575